187. On the Macrolactonization of β-Hydroxy Acids. Crystal Structures of the Pentolide and the Hexolide from (*R*)-3-Hydroxybutanoic Acid. Molecular Modeling Studies of the Tetrolide

by **Dieter Seebach***, **Urs Brändli**[1]), **Hans-Martin Müller**, **Max Dobler**, and **Martin Egli**

Laboratorium für organische Chemie der Eidgenössischen Technischen Hochschule, ETH-Zentrum, Universitätstrasse 16, CH–8092 Zürich

and **Michael Przybylski** and **Klaus Schneider**

Fakultät für Chemie der Universität Konstanz, Universitätsstrasse 10, D–7750 Konstanz

Dedicated to Prof. Dr. *Wilhelm Simon* on the occasion of his 60th birthday

(27.VII.89)

The temperature and concentration dependence of the previously reported formation of oligolides from (*R*)- or (*S*)-3-hydroxybutanoic acid under *Yamaguchi*'s macrolactonization conditions (2,4,6-trichlorobenzoyl chloride/base) was studied. While the content of hexolide **2** in the product mixture is almost invariably *ca.* 35%, the amounts of pentolide **1** and of the larger rings strongly depend upon the temperature employed (*Fig. 1*). Cyclic oligomers (**5,6**) are also obtained from 3-hydroxypentanoic acid. Enantiomerically pure β-butyrolactone can be used for the preparation of pento-, hexo-, and heptolide under *Shanzer*'s macrolactonization conditions (tetraoxadistannacyclodecane 'template'). The X-ray crystal structures of the pentolide **1** and of two modifications (space groups *C* 2 and *P* 2_1) of the hexolide **2** were determined (*Figs. 2–6* and *Tables 1* and *5*). No close contacts between substituent atoms and atoms in the rings or between ring atoms are observed in these structures. The hexolide *C* 2 modification is 'just a large ring', while the crystals of the *P* 2_1 modification contain folded rings the backbones of which resemble the seam of a tennis ball. A comparison of the torsion angles in the folded hexolide ring of the *P* 2_1 modification with those in the helical poly-(*R*)-3-hydroxybutanoate (PHB) suggests (*Table 2*) that the same interactions might be responsible for folding in the first and helix formation in the second case. Molecular modeling with force-field energy minimization of the tetrolide from four homochiral β-hydroxybutanoic acid units was undertaken, in order to find possible reasons for the fact that we failed to detect the tetrolide in the reaction mixtures. The calculated conformational energies (per monomer) for some of the tetrolide models (*Figs. 7–9* and *Tables 3* and *4*) are not significantly higher than for the pentolide and hexolide crystal structures. We conclude that thermodynamic instability is an unlikely reason for the lack of tetrolide isolation. This result and failure to observe equilibration of pentolide **1** to a mixture of oligomers under the reaction conditions suggest that product distribution is governed by kinetic control.

A) Introduction and Motivation. – We reported recently that treatment of enantiomerically pure 3-hydroxybutanoic acid under *Yamaguchi*'s macrolactonization conditions yields macropento-, macrohexo-, and macroheptolides **1–3**, respectively, in a surprisingly good total yield of *ca.* 50%, but that we were unable to detect the corresponding macrotetrolide [1a]. In view of the importance of poly-[(*R*)-3-hydroxybutanoate] (PHB), a biodegradable polymer obtained by fermentation, containing a high degree of crystalline domains which consist of a helical arrangement [1b], it was interesting to investi-

[1]) Part of the Ph. D. thesis of *U. B.*, ETH-Zürich, No. 8680, 1988.

gate the scope and limitations of this cyclization, to determine the structures of the small cyclic oligomers of hydroxybutanoic acid, and to use structural parameters thus obtained for modeling experiments which might reveal reasons for the lack of isolation of a macrotetrolide.

B) Preparative Results. – First, we studied the influence of the temperature on the ring size of the formed macrocycles, *cf.* the macrocyclizations of bicyclic acetals under the influence of $BF_3 \cdot Et_2O$ [2], of (hydroxymethyl)furancarboxylic acids under *Mukaiyama*'s chloropyridinium-salt conditions [3][2]), and of bis-tosylamides with dihalides to give

Scheme

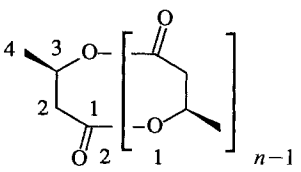

1 $n = 5$, **2** $n = 6$, **3** $n = 7$

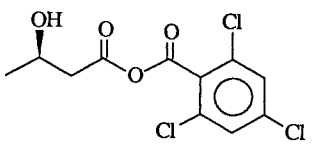

4

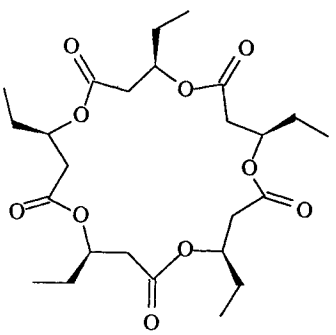

5

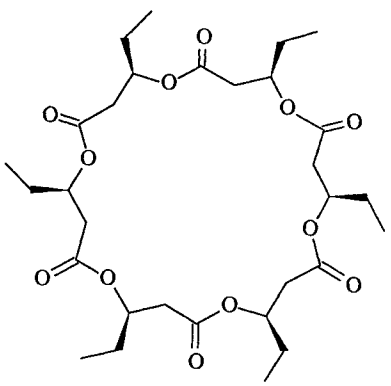

6

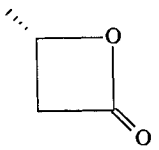

7

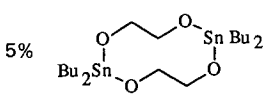

8

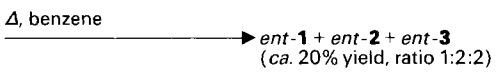

[2]) In some of the cases [2] [3], the composition of the product mixture strongly depends upon the choice of solvent and upon the product solubilities (thermodynamic control). Another macrocyclization occurring in good yields in homogeneous solutions and in the absence of templating metal ions is the synthesis of cryptophanes [4].

azamacrocycles [5]. In our case, the mixed anhydride **4** was generated under normal-concentration conditions, and cyclization was induced by treatment with *Steglich* base [= 4-(dimethylamino)pyridine] under high-dilution conditions in benzene or toluene [6], the cyclization products being in solution at all times under the conditions employed[3]).

Cyclization of the hydroxybutanoic acid does not occur *via* the β-lactone, because the submission of (*S*)-β-butyrolactone to *Yamaguchi*'s macrolactonization conditions[4]) led only to the formation of polymeric material, but not of oligomeric cyclic products. While there was hardly any effect of concentration (0.5M, 0.05M, and 0.025M runs gave essen-

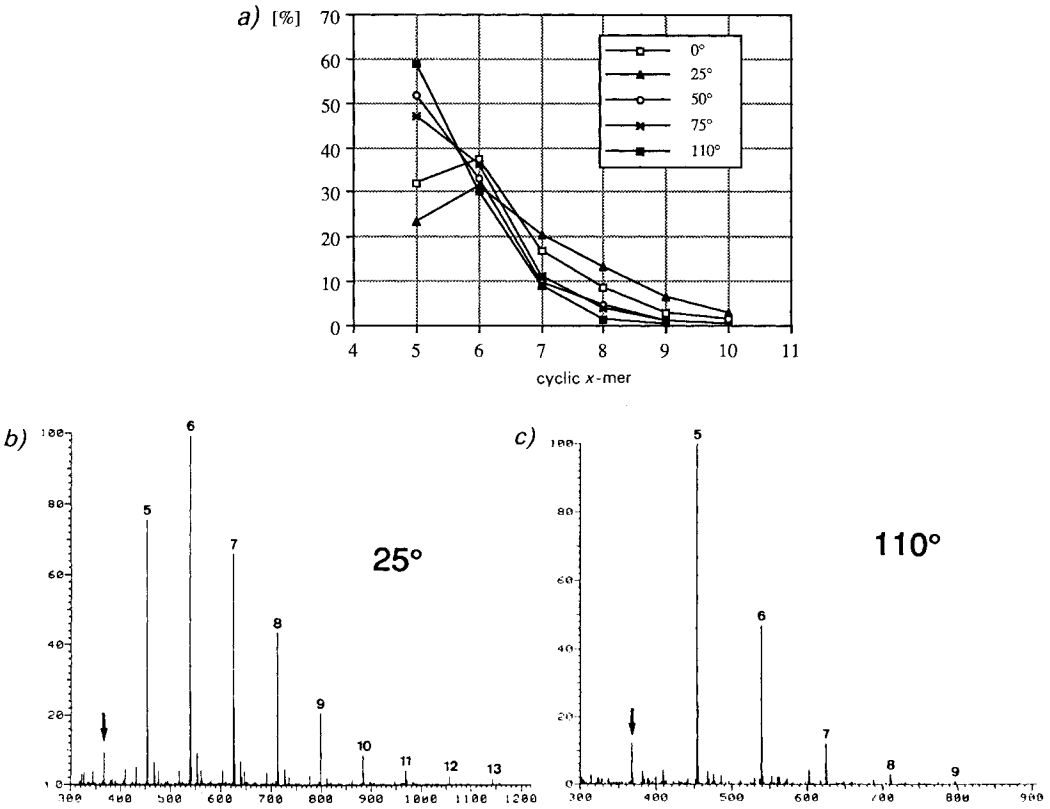

Fig. 1. *Distribution of cyclic oligomers from* Yamaguchi *macrolactonization.* a) *Plot of relative amounts of cyclic oligomers as a function of temperature.* b) and c) *Crude-product FAB-MS after reaction at 25° and 110°, respectively.* The spectra were obtained by NaI-spiked FAB-MS measurements with a *Finnigan-AMD/MAT-312,* using a tetraethyleneglycol (TEG) matrix as described in [1a]. The arrow in *b* and *c* points to the mass peak of the tetramer, which was shown to arise from an open-chain ion by linked-scan metastable-ion MS [1a].

[3]) Precipitates separated from the reaction mixture contain only the (dimethylamino)pyridinium salt of trichlorobenzoic acid, but no cyclization products in detectable amounts.

[4]) A highly dilute solution of *Steglich* base in toluene was slowly added to a solution of the β-lactone in the same solvent; only polymeric material was isolated.

tially the same oligomer composition under otherwise identical conditions)[5]), change of temperature from 0 to 110° had a pronounced effect. The fraction of smaller rings increases with rising temperature (see *Fig. 1*, a). It is remarkable that the formation of cyclic hexamer **2** (*ca.* 1/3 of the total cyclic products) is nearly independent upon the temperature. Using the same MS technique as described in [1a], we did not detect the cyclic tetramer in the samples obtained unter the various reaction conditions. The product distribution is most likely the result of kinetic control, since we did not find other cyclic oligomers after having exposed the pentamer **1** to the reaction conditions[6]). To find out whether the macrocycles of type **1**–**3**, which have been shown not to complex alkali ions selectively [1a][7]), associate with a component of the ammonium benzoate formed concomitantly, we recorded their 300-MHz ^{1}H-NMR spectra in the absence and presence of this salt, to find that there was no difference.

To see whether other β-hydroxy acids can be converted to analogous macrocycles, we had already checked (*R*)-trifluoro-3-hydroxybutanoic acid without success [1][7], and we have now found that the trichloroderivative [7][8] also did not yield macrocycles. More surprisingly, an experiment with simple β-hydroxypropanoic acid did not lead to detectable cyclic products. On the other hand, the more lipophilic (*R*)-3-hydroxypentanoic acid [9], when treated under *Yamaguchi*'s macrolactonization conditions, gave rise to the cyclic pentamer **5** and hexamer **6**, each isolated in 10% yield.

Finally, it is noteworthy that *Shanzer*'s method [10] of macrocyclization in the presence of 5% tetraoxadistannacyclodecane **8** when applied to (−)-(*S*)-β-butyrolactone (**7**) led to the isolation of the three enantiomeric oligomers *ent*-**1**, *ent*-**2**, and *ent*-**3** in *ca.* 20% yield[8])[9]) (see the *Scheme*). This macrolactonization occurs mainly with retention of configuration, as expected. While a tetrolide is formed (12%) form β-propiolactone in the distannoxane-mediated cyclization [10], we again failed to detect one in the present case. Hoping that we might learn about possible reasons for the observed oligolide distributions, we decided to determine crystal structures of some of the cyclic oligomers **1**–**3** and to perform a conformational analysis of the tetrolide with force-field methods.

C) X-Ray Crystal Structure Analyses of the Pentolide 1 and the Hexolide 2. – We wanted to see whether crystal structure analyses of **1** and **2** would reveal any structural

---

[5]) A run performed with $5 \cdot 10^{-4}$ M concentration did not furnish any cyclic products as judged by FAB-MS.

[6]) A solution of 0.1 mmol of pentamer **1**, 1 g of *Steglich* base, and 0.1 mmol of mixed anhydride from 3-hydroxybutanoic and trichlorobenzoic acid in 100 ml of toluene was stirred at room temperature for 4.5 h; besides pentamer, no other cyclic oligolides were detected by TLC.

[7]) There was no difference in the relative peak heights of the different cyclic oligomers depending upon the method of ionization ($(M + H^+)$, $(M + Na^+)$, $(M + Cs^+)$). Also, embedding the hexamer **2** into a PVC film did not lead to an ion-transporting membrane (Na^+, K^+, Ca^{2+}, Mg^{2+}). We thank Prof. *W. Simon* and *M. Müller* for carrying out these experiments.

[8]) This is half the yield obtained with *Yamaguchi*'s method, but the reaction is carried out more easily (less highly diluted solution) and might be more suitable for larger-scale preparations of the macrocycles of type **1**–**3**. The so-called template-catalyst **8** is readily obtained by mixing ethyleneglycol and dibutyldichlorotin in benzene [11]. According to the value of optical rotation of the samples obtained, partial racemization may have occurred on the way from **7** to *ent*-**2**.

[9]) It is known that racemic β-butyrolactone, when polymerized with a chiral *Lewis*-acid catalyst undergoes partial resolution, with one enantiomer enriched in the polymeric chain, the other in the unreacted lactone monomer fraction (see the ref. given in a recent review article on kinetic resolution [12]).

Table 1. *Crystal Data for the Pentolide* **1** *and the Two Modifications of the Hexolide* **2**

	1	**2** (mod. $C2$)	**2** (mod. $P2_1$)
Formula	$C_{20}H_{30}O_{10}$	$C_{24}H_{36}O_{12}$	$C_{24}H_{36}O_{12}$
Molecular weight	430.46	516.54	516.54
Space group	$P2_12_12_1$	$C2$	$P2_1$
a [Å]	9.619(3)	19.826(11)	10.090(5)
b [Å]	9.763(1)	5.550(3)	15.622(11)
c [Å]	24.833(5)	12.938(7)	18.265(10)
β [°]	–	97.84(5)	98.38(6)
V [Å^3]	2332.1	1410.2	2848.4
Z	4	2	4
d_x [g/cm^3]	1.23	1.22	1.21
Range measured	0–27°	0–25°	0–25°
Reflections measured	2890	1381	5195
Reflections used ($I > 3\sigma[I]$)	1379	874	3393
Final R (unweighted)	0.045	0.13	0.043

reasons for the observed absence of tetrolide in the reaction mixture. Suitable crystals can easily be obtained from $CHCl_3$ by slow evaporation of the solvent. Crystal data for the structures are given in *Table 1*.

The pentolide **1** crystallizes in the orthorhombic space group $P2_12_12_1$. The molecule adopts a rather flat disk-like conformation with four carbonyl O-atoms on one and the fifth on the opposite side of a mean molecular plane (*Fig. 2*). The ester groups are in the expected antiperiplanar conformation, the corresponding torsion angle being almost 180°.

For the hexolide **2**, two different crystal modifications could be isolated from the same batch. The first modification is monoclinic, space group $P2_1$, and has two independent molecules in the asymmetric unit. Both molecules have the same conformation and are almost superimposable. As in the pentolide, all ester groups are antiperiplanar, the corresponding torsion angle being almost 180°. The ring shape can best be described as resembling the seam of a tennisball *(Fig. 3)*. Similar conformations were observed for some alkali-metal complexes of other macrocyclic compounds [14], *i.e.* for nonactin [15].

The conformation of **2** ($P2_1$ modification) is quite compact, with no internal cavity, as can be seen in *Fig. 5*, showing a 'dotted surface' representation of the *van der Waals* surface of the molecule. It is interesting to note that this conformation bears a certain relationship to the structure of linear (*R*)-polyhydroxybutanoic acid (PHB), which forms a helix with a pitch of 5.96 Å [16]. Two hydroxybutanoic-acid monomers, symmetry-related by a twofold screw axis along the helix axis, constitute one turn of the helix. The sequence of torsion angles along such a turn is similar to two stretches in the hexolide structure *(Table 2)*.

The second crystal modification of the hexolide **2** is also monoclinic, but crystallizes in the space group $C2$. The molecule has a completely different conformation with a crystallographic twofold rotation axis. Its shape is nearly rectangular, with sides of 8.6 Å (O(2)···O(2′)) and 5.5 Å (O(6)···O(6′)). The carbonyl O-atoms lie alternately above and below the mean molecular plane *(Fig. 4)*.

As in the $P2_1$ modification, the conformation of **2** in the $C2$ modification is quite compact with no discernible internal cavity *(Fig. 6)*.

Fig. 2. *ORTEP* [13] *stereoview of the pentolide* **1**, *showing the disk-like conformation.* The O-atoms are numbered.

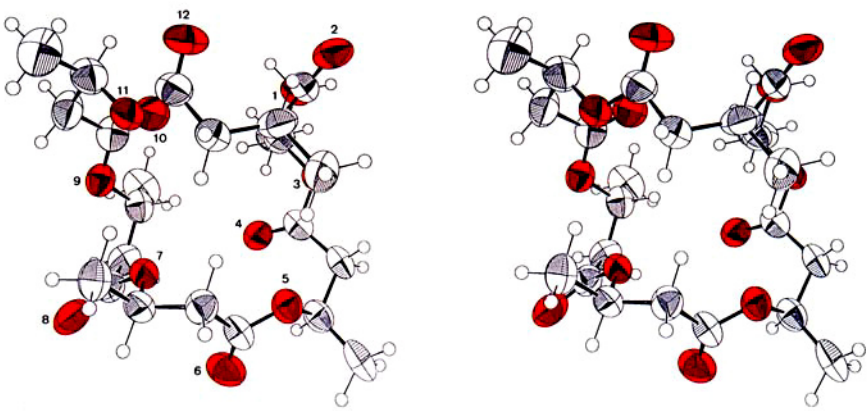

Fig. 3. *ORTEP* [13] *stereoview of the hexolide* **2** *in the* $P2_1$ *modification.* The shape of the ring resembles the seam of a tennis ball. The second, crystallographically independent molecule has an almost identical conformation. The O-atoms are numbered.

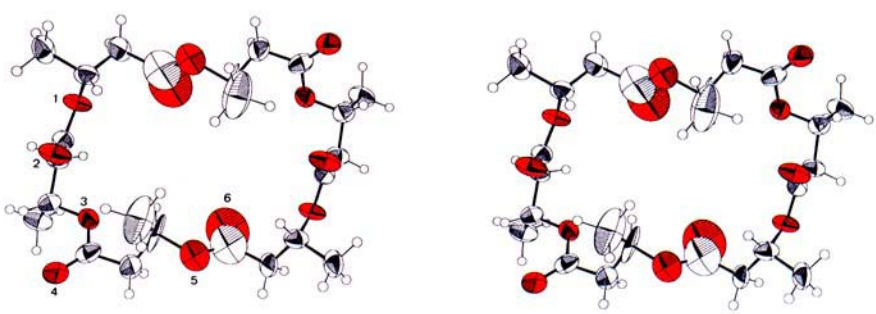

Fig. 4. *ORTEP* [13] *stereoview of the hexolide* **2** *in the* C2 *modification.* Note the elongated thermal ellipsoids of some atoms, possibly indicating a certain disorder. The O-atoms of an asymmetric unit are numbered.

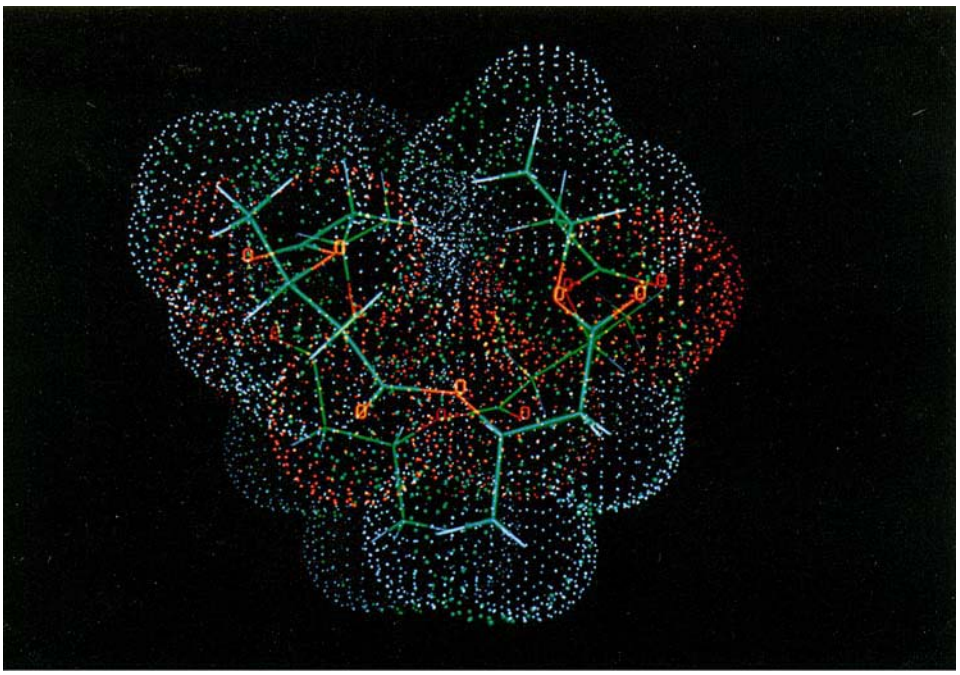

Fig. 5. *'Dotted surface' representation of the hexolide* **2** ($P2_1$ modification), *showing the compact conformation with no internal cavity*

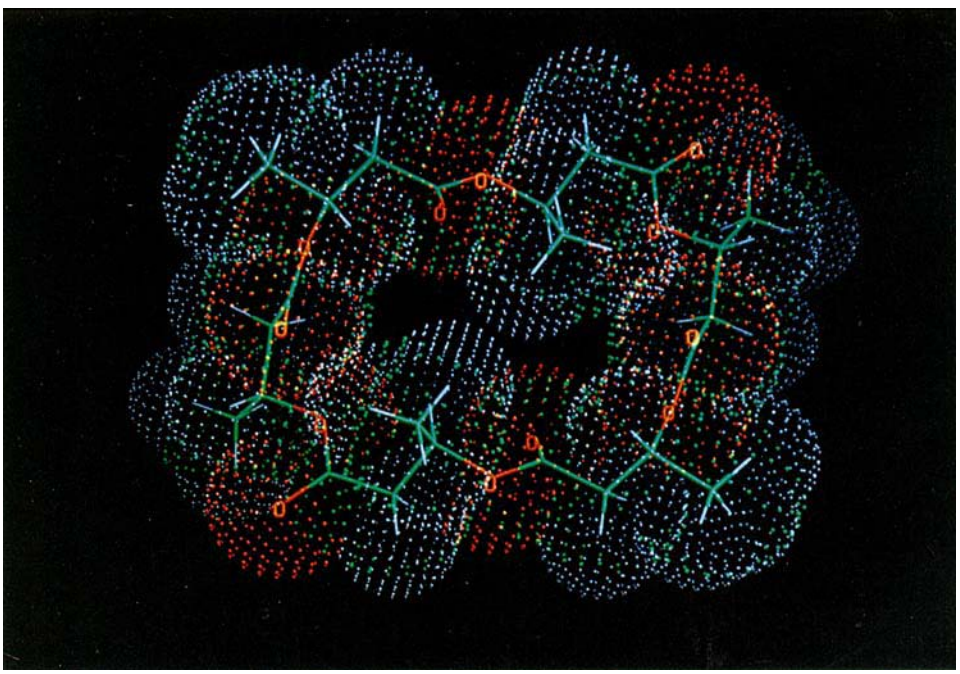

Fig. 6. *'Dotted surface' representation of the hexolide* **2** ($C2$ modification), *showing the compact, rectangular conformation with no internal cavity*. The view is along the crystallographic twofold rotation axis.

Table 2. *Similarity of Torsion Angles in the Helical Polyhydroxybutanoic Acid (PHB)* [16d] *and in Two Stretches of the Hexolide* **2** *in its* $P2_1$ *Modification*

	PHB	Stretch 1	Mol. 1	Mol. 2	Stretch 2	Mol. 1	Mol. 2
CH_2–$CH(CH_3)$	−52.0	C(22)–C(23)	−58.2	−65.5	C(10)–C(11)	−59.9	−61.2
$CH(CH_3)$–O	151.8	C(23)–O(1)	138.2	143.9	C(11)–O(7)	151.4	155.2
O–CO	−175.2	O(1)–C(1)	−176.1	177.6	O(7)–C(13)	−170.9	−175.0
CO–CH_2	−46.5	C(1)–C(2)	−21.1	−19.1	C(13)–C(14)	−44.2	−39.5
CH_2–$CH(CH_3)$	−52.0	C(2)–C(3)	−58.5	−62.1	C(14)–C(15)	−49.8	−54.0
$CH(CH_3)$–O	151.8	C(3)–O(3)	155.5	154.9	C(15)–O(9)	159.8	159.7
O–CO	−175.2	O(3)–C(5)	−176.1	−173.7	O(9)–C(17)	−171.9	−174.0

All structures have some common features. As already mentioned, all ester groups are in the usual antiperiplanar arrangement. The C–CO–O–C torsion angles deviate only slightly from 180°, the maximum deviation is 5.7° for the pentolide **1** and 11.4° and 10.9° for the $P2_1$ and 5.7° for the $C2$ modification, respectively, of the hexolide **2**. In esters of secondary alcohols, the optimal torsion angles CO–O–CH–C(β) are (±)120° to avoid – given a planar ester group – short 1···5 contacts from the carbonyl O- to the C(β)-atoms. This makes the H-atom in α-position coplanar with the ester group, a fact first mentioned by *Mathieson* [17] and later studied quantitatively [18]. Because of the ring-closure conditions in the pentolide and hexolide conformations, this requirement cannot be strictly fulfilled. The observed torsion angles CO–O–CH–CH_3 are in the range of − 80.5° to − 142.9°, those for CO–O–CH–CH_2 of 98.1° to 159.8°. A list of ring torsion angles for all structures is given in the *Exper. Part (Table 5)*.

D) Molecular-Modeling Studies of the Tetrolide. – The observed ring conformations in the pentolide and hexolide structures **1** and **2**, respectively, give no direct structural indication why a tetrolide could not exist. We, therefore, attempted to build models of the tetrolide. Of the 16 ring torsion angles, the four C–CO–O–C angles of the ester groups can be fixed at 180°. Of the four CO–O–$CH(CH_3)$–CH_2 torsion angels, we know that in **1** and **2** they are restricted to a range of *ca.* 100° to 160°. Only the remaining eight torsion angles are more or less free. Using these guidelines, it was quite easy to build a possible tetrolide model (*Fig. 7*, model **A**). It has near fourfold rotation symmetry, with all C=O groups on the same side of a mean molecular plane, and the Me groups at the corners pointing to the outside. Unfavourable nonbonded contacts are avoided, but at the cost of a parallel arrangement of four dipoles and rather short distances between the carbonyl O-atoms. An alternative model (*Fig. 7*, model **B**) with C=O groups alternatingly up and down has CO–O–$CH(CH_3)$–CH_2 torsion angles of *ca.* 180°, which makes the 1···5 distances from carbonyl O-atoms to the Me groups rather short. A third model (*Fig. 7*, model **C**) was built starting with the crystal structure of the 3-hydroxypropanoic-acid tetramer [10] and adding four Me groups. Like model **B**, it suffers from short C=O···CH_3 contacts. To further probe conformational space, we generated models with random values for the 12 variable torsion angles (a better way to do this is described in [19]). Of the $5 \cdot 10^5$ generated sets, 21 were close to a cyclic conformation and were subsequently used.

To put these models on a more quantitative basis, they were optimized with the force field program AMBER [20], using their all-atom force field [21]. This force field has no

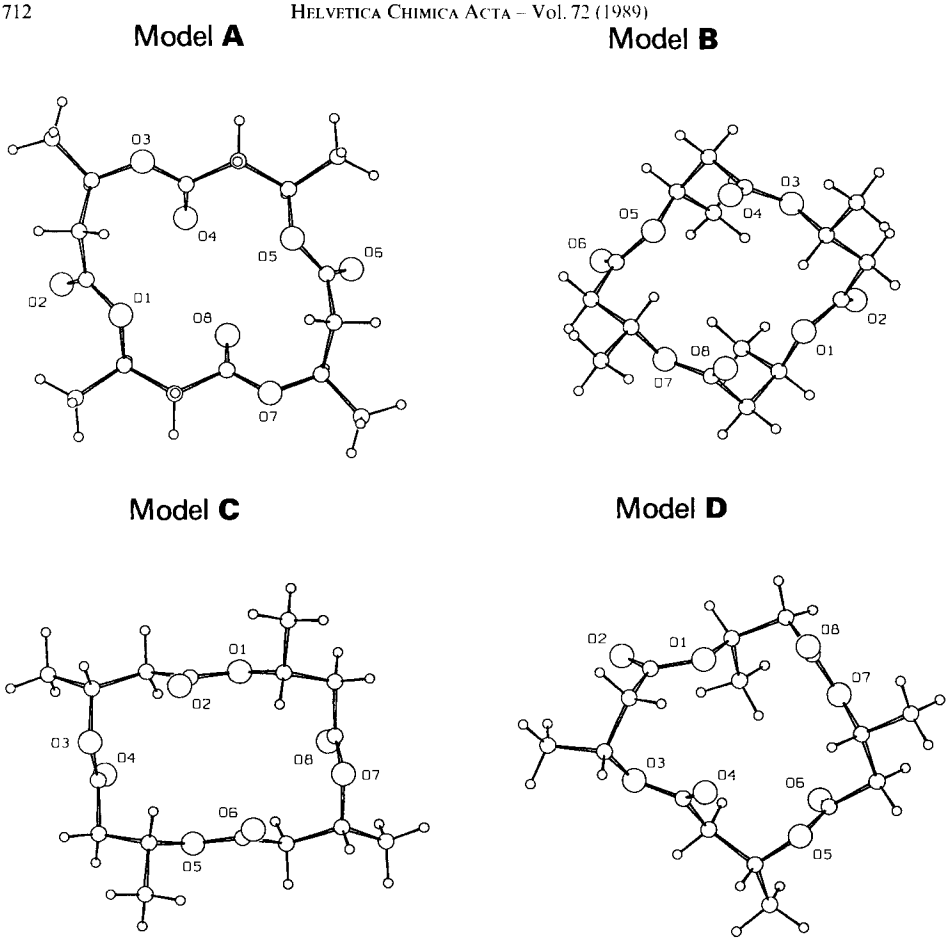

Fig. 7. *Conformations of four tetrolide models after optimization by force-field methods.* Models **A** and **B** were initially visually built on a graphics computer using standard bond lengths and angles and planar ester groups, model **C** corresponds to the crystal structure of 3-hydroxypropanoic acid [10] with four Me groups added geometrically, and model **D** is the best of the computer-generated models with random torsion angles.

Table 3. *Force Constants* [kcal/mol] *for Ester Groups*[a])

Bond	K_r	r_o	Angles	K_θ	θ_o	Torsion
C–OS	450.0	1.340	OS–C–O	80.0	123.4	OS–O–C–CT $V_n = 10.5$ $n = 2$ $\gamma = 180.0$
			OS–C–CT	70.0	111.2	
			C–O–CT	100.0	117.4	
			C–CT–OH	50.0	109.5	
			CA–CT–OH	50.0	109.5	

[a]) All other force constants are those from the all-atom force field [21]. The equilibrium values for bond lengths and angles are taken from the statistical survey of the geometry of ester groups [18a]. The atom types correspond to standard AMBER terminology [20].

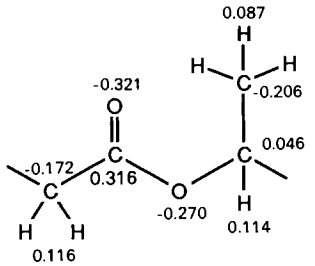

Fig. 8. *Partial charges used for the macrolide monomers in the force-field optimizations* (program AM1 [22])

parameters for ester groups; therefore, the force constants given in *Table 3* were added. Partial charges were calculated with the program AM1, a parametric quantum mechanical molecular model program based on the NDDO approximation [22] (see *Fig. 8*). All calculations were performed on the Cray X-MP of the ETH Zürich. In addition to the tetrolide models, the crystal-structure conformations of the pentolide and of the hexolide were also optimized (see *Exper. Part, Table 5*).

The results for the pentolide **1**, two hexolide modifications **2**, and tetrolide models **A**, **B**, **C**, and the six best of the 21 tetrolide models generated with random torsion angles are given in *Table 4*. For comparison, *Fig. 9* shows the energies for a monomer, *i.e.* divided by the number of residues[10]).

It is evident that all tetrolide models have higher potential energies than the pentolide and hexolide structures. On the other hand, the tetrolide model with the lowest energy, **B**, has no obvious strained features, and none of the partial energy contributions differs very

Table 4. *Potential Energy of Optimized Hexolide, Pentolide, and Some Tetrolide Conformations*[a])

	Energy							
	Total	Bond	Angle	Torsion	Nonbonded		Electrostatic	
					>1···4	1···4	>1···4	1···4
Hexolide **2** ($P2_1$)	–7.49	0.56	2.82	4.62	–11.34	9.47	43.55	–57.18
Hexolide **2** ($C2$)	–6.87	0.58	3.25	3.55	–6.48	8.45	40.25	–56.47
Pentolide **1**	–3.60	0.46	3.49	4.93	–6.65	7.19	33.75	–46.77
Model **B**	–1.19	0.58	3.16	2.17	–4.56	5.47	30.52	–38.52
Model **C**	–0.48	0.54	4.19	1.61	–4.06	5.04	30.69	–38.48
Model *12* (= **D**)	1.23	0.56	4.11	3.10	–5.31	5.67	31.95	–38.85
Model **A**	2.94	0.47	2.56	7.06	–5.03	6.18	28.75	–37.05
Model *13*	3.15	0.57	3.28	7.17	–4.28	6.22	27.96	–37.76
Model *14*	3.77	0.55	2.30	9.41	–5.61	6.77	27.88	–37.52
Model *6*	4.42	0.61	5.05	6.61	–4.96	5.90	29.75	–38.54
Model *16*	4.90	0.67	3.21	9.03	–5.99	6.68	29.03	–37.72
Model *15*	7.63	0.72	6.84	4.67	–3.52	4.97	32.74	–38.79

[a]) All calculations were done with the program AMBER [18] using an all-atom force field [19]. All energies in kcal/mol.

[10]) This is of course not quite correct because the number of nonbonded interactions is not a linear function of the number of monomers. The number of nonbonded interactions per monomer is 219 for the tetrolide, 291 for the pentolide and 363 for the hexolide.

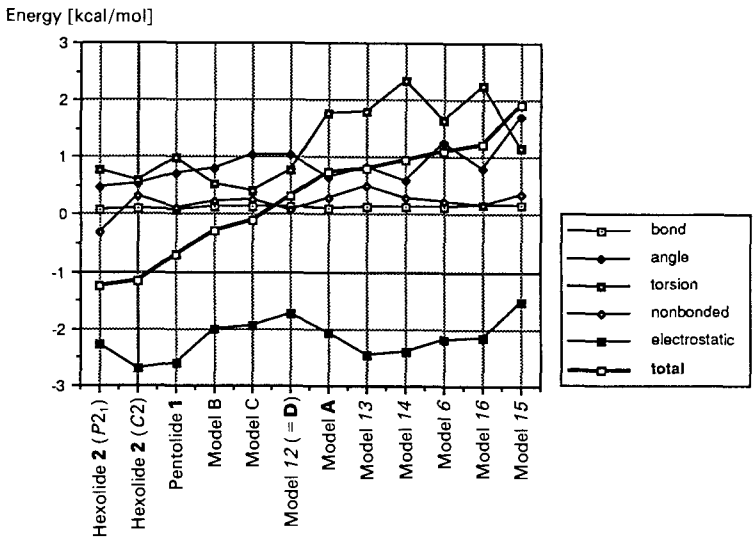

Fig. 9. *Results of force-field optimizations for the pentolide* **1**, *hexolide* **2**, *and tetrolide models* **A**, **B**, **C** *and the best six of the computer-generated tetrolide models using random torsion angles.* Energies (kcal/mol) are divided by the number of monomers in the different models.

much from those found in the pentolide and hexolide structures. The force field calculations do not give conclusive evidence that structural reasons forbid the formation of a tetrolide. It may be that the potential energy from hexolide to pentolide to the lowest-energy model of the tetrolide crosses a borderline between pentolide and tetrolide. For the pentolide, there may be enough variable parameters in the molecule, so that small adjustments to them suffice to produce a reasonably strain-free conformation. The smaller ring size of the tetrolide may necessitate adjustments to bond angles and torsion angles that make ring closure during the chemical reaction energetically unfavourable so that the larger rings are preferred, that is to say that a tetrahedral intermediate of type **9** may be highly strained but not the corresponding tetrolide.

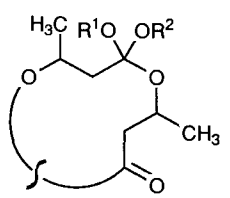

9

Experimental Part

General Procedure for the Evaluation of Temperature Dependence [1]. To a stirred soln. of 0.5 g (4.8 mmol) of (*R*)-3-hydroxybutanoic acid in 10 ml of THF at 0° was slowly added Et_3N (0.87 ml, 6.2 mmol) and 2,4,6-trichlorobenzoyl chloride (0.67 ml, 4.8 mmol). After 30 min, the ice-bath was removed, and the temp. was allowed to rise within 1.5 h from 0° to r.t. The suspension was filtered and the filtrate diluted with 10 ml of toluene. This soln. was added over 4 h (with a motor-driven syringe) under Ar to a stirred soln. of 4-(dimethylamino)pyridine (3.52 g, 28.8 mmol, 6 equiv.) in toluene (200 ml) at different temp. Stirring was continued for 30 min. The mixture was then diluted with 100 ml of Et_2O and washed with 100 ml portions of 1N HCl, sat. $NaHCO_3$ soln., and sat. NaCl soln. From these crude product mixtures, the FAB-MS were measured.

Preparation of the Macrolides **5** *and* **6**. The general procedure (employed at 50°) with 0.57 g (4.8 mmol) of (*R*)-3-hydroxyvaleric acid gave, after FC (Et_2O/Petroleum ether 7:3), 69 mg (12%) of **5** and 50 mg (9%) of **6**.

(4R,8R,12R,16R,20R)-4,8,12,16,20-Pentaethyl-1,5,9,13,17-pentaoxacycloicosane-2,6,10,14,18-pentone (**5**). M.p. 111–112°. $[\alpha]_D^{r.t.} = +17.9$ ($c = 1.43$, $CHCl_3$). IR ($CHCl_3$): 2970*w*, 1740*s*, 1460*w*, 1385*w*, 1170*m*. ^{1}H-NMR (300 MHz, $CDCl_3$): 5.10–5.21 (*m*, 5 CH_3CH_2CHO); 2.42–2.62 (*m*, 5 CH_2CO); 1.50–1.75 (*m*, 5 CH_3CH_2); 0.92 (*t*, $J = 7.5$, 5 CH_3). FAB-MS: 501 (3, $[M+1]^+$), 277 (5), 201 (3), 186 (4), 185 (60), 183 (6), 101 (12), 93 (100), 83 (22), 75 (27), 57 (22), 45 (16). Anal. calc. for $C_{25}H_{40}O_{10}$ (500.6): C 59.98, H 8.05; found: C 59.77, H 8.08. Mol.wt. (osmom.): 509.

(4R,8R,12R,16R,20R,24R)-4,8,12,16,20,24-Hexaethyl-1,5,9,13,17,21-hexaoxacyclotetracosane-2,6,10,14,18,22-hexone (**6**). M.p. 94–95°. $[\alpha]_D^{r.t.} = +19.2$ ($c = 0.93$, $CHCl_3$). IR ($CHCl_3$): 2985*w*, 2940*w*, 2880*w*, 1740*s*, 1460*w*, 1380*w*, 1340*w*, 1180*s*, 1040*w*, 1080*w*, 970*w*. ^{1}H-NMR (300 MHz, $CDCl_3$): 5.17–5.31 (*m*, 6 CH_3CH_2CHO); 2.45–2.66 (*m*, 6 CH_2CO); 1.55–170 (*m*, 6 CH_3CH_2); 0.90 (*t*, $J = 7.5$, 6 CH_3). FAB-MS: 601 (3, $[M+1]^+$), 301 (7), 283 (2), 201 (11), 185 (32), 183 (22), 101 (48), 93 (74), 83 (100), 75 (21), 57 (28), 55 (38), 45 (18), 43 (16), 41 (11), 29 (13). Anal. calc. for $C_{30}H_{48}O_{12}$ (600.72): C 59.98, H 8.05; found: C 59.91, H 8.23. Mol. wt. (osmom.): 597.5.

Cyclization of (S)-β-Butyrolactone by Shanzer's *Method.* In a 500-ml one-necked round bottom flask, (*S*)-β-butyrolactone (3 g, 34.8 mmol) [23] and 1,1,6,6-tetrabutyl-1,6-distanna-2,5,7,10-tetraoxacyclodecane [11] (300 mg, 0.17 mmol) were refluxed in 240 ml of benzene overnight. The resulting slightly yellow mixture was evaporated, and FC (Et_2O/hexane 7:3) of the viscous crude product gave 152 mg (5%) of pentolide *ent*-**1**, 282 mg (9%) of hexolide *ent*-**2**, and 311 mg (10%) of heptolide *ent*-**3**. The spectra of these compounds were identical with the ones described in [1a].

In an analogous run using toluene instead of benzene, the resulting crude product was separated from polymers by FC (Et_2O/pentane 2:1) without separation of oligomers, the oligomeric mixture thus obtained was separated by FC (Et_2O/pentane 2:1). All fractions containing the hexolide *ent*-**2** were collected. Evaporation of the solvent gave 24 mg (0.8%) of a colorless solid. $[\alpha]_D^{r.t.} = -8.2$ ($c = 1.37$, $CHCl_3$). Enantiomerically pure **2**: $[\alpha]_D^{r.t.} = +11.1$ ($c = 1.52$, $CHCl_3$) in [1a]; $[\alpha]_D^{r.t.}$ of **3** = +7.3 ($c = 1.09$, $CHCl_3$).

X-Ray Crystal Structures. Crystal data for the three structures are given in *Table 1*. Reflection intensities were measured with a four-circle diffractometer *(Enraf-Nonius CAD4)* using graphite monochromatized MoK_α radiation (0.7107 Å). The three structures were solved by direct methods with SHELXS-86 [24].

Pentolide **1**. C- and O-atoms were refined anisotropically with SHELX76 [25]. The full-matrix least-squares analysis using calculated H-atoms riding on the corresponding C-atoms (C–H distance 1.08 Å) and constraining their isotropic displacement parameters to 120% of the expression $(U_{11} + U_{22} + U_{33})/3$ of the attached C-atoms converged at a final *R* factor of 0.045 (with unit weights).

Hexolide **2** (*C*2 modification). During initial refinement, the high values of some isotropic displacement parameters indicated a disorder in one of the ester groups (atoms O(5), O(6), and C(9)). These atoms and the two neighbouring C-atoms were removed. In a subsequent difference *Fourier* map, an ester fragment with reasonable arrangement (antiperiplanar conformation, the corresponding torsion angle being almost 180°) but poor geometry could be located. It was refined with soft constraints (planar; C(9)–O(6), 1.180 Å; O(5)–C(9), 1.340 Å; C(9)–C(10), 1.530 Å), using restricted isotropic displacement parameters for atoms O(5), O(6), and C(9) ($U = 0.10$, 0.25, and 0.17 resp.). The H-atom positions were calculated and treated as in the pentolide. The final *R* factor was 0.13.

Hexolide **2** ($P2_1$ modification). The structure was refined isotropically by full-matrix least-squares analysis with SHELX76 [25]. Due to the large number of parameters, the anisotropic refinement was performed with the X-RAY system [26]. The H-atom positions were calculated after four cycles of anisotropic refinement (C–H distances 1.08 Å). After three additional full-matrix cycles for C- and O-atoms, the positions of the H-atoms were redetermined. A final structrure factor calculation, restricting the isotropic displacement parameters of the H-atoms as above resulted in a final *R* factor of 0.043.

Ring torsion angles for the three structures are given in *Table 5*. A full list of coordinates with displacement parameters as well as bond lengths and angles is available from the authors.

Table 5. *Ring Torsion Angles in the Crystal Structures of Pentolide* **1** *and the Two Modifications of Hexolide* **2**, *and Torsion Angles in the Calculated Models* (AMBER [18])[a])

	Pentolide **1**			Hexolide **2** ($P2_1$)			Hexolide **2** ($C2$)	
	obs.	calc.		mol. 1	mol. 2	calc.	obs.	calc.
O(1)–C(1)	–176.0	–179.0	O(1)–C(1)	–176.1	177.6	–179.9	179.7	175.5
C(1)–C(2)	58.1	58.8	C(1)–C(2)	–21.2	–19.1	–46.7	168.4	151.8
C(2)–C(3)	173.3	172.9	C(2)–C(3)	–58.5	–62.2	–55.4	–69.2	–65.5
C(3)–O(3)	99.8	80.5	C(3)–O(3)	155.5	154.9	165.1	151.5	160.9
O(3)–C(5)	179.3	–173.1	O(3)–C(5)	–176.1	–173.7	–173.6	180.0	–177.9
C(5)–C(6)	–70.6	–58.4	C(5)–C(6)	158.4	164.1	143.0	50.6	47.3
C(6)–C(7)	–64.5	–68.5	C(6)–C(7)	–62.9	–63.4	–57.3	169.5	174.1
C(7)–O(5)	98.1	93.9	C(7)–O(5)	142.5	140.6	161.2	116.1	71.3
O(5)–C(9)	178.0	–178.2	O(5)–C(9)	–168.6	–169.1	–172.2	174.3	–173.7
C(9)–C(10)	174.1	170.6	C(9)–C(10)	145.7	145.1	120.3	–99.7	–74.1
C(10)–C(11)	–67.3	–65.4	C(10)–C(11)	–59.9	–61.2	–53.3	–79.1	–72.5
C(11)–O(7)	144.8	155.8	C(11)–O(7)	151.4	155.1	164.1	152.4	166.5
O(7)–C(13)	–174.3	–176.0	O(7)–C(13)	–170.9	–175.0	–178.3		175.4
C(13)–C(14)	172.8	150.9	C(13)–C(14)	–44.2	–39.4	–51.4		151.7
C(14)–C(15)	–169.3	–160.5	C(14)–C(15)	–49.8	–54.0	–53.0		–65.4
C(15)–O(9)	132.0	164.0	C(15)–O(9)	159.8	159.7	164.3		161.1
O(9)–C(17)	–175.9	–179.1	O(9)–C(17)	–171.9	–174.0	–172.7		–177.8
C(17)–C(18)	135.2	107.3	C(17)–C(18)	141.2	151.8	139.7		47.4
C(18)–C(19)	–62.1	–58.4	C(18)–C(19)	–55.4	–57.8	–55.1		173.9
C(19)–O(1)	155.3	162.0	C(19)–O(11)	149.6	136.1	161.4		71.1
			O(11)–C(21)	178.0	–170.1	–172.3		–173.9
			C(21)–C(22)	141.6	151.7	121.7		–74.2
			C(22)–C(23)	–58.2	–65.5	–56.4		–72.4
			C(23)–O(1)	138.2	143.9	165.5		166.6

[a]) Mean differences [Å] in the coordinates of experimental and calculated structures are: pentolide **1** (0.087, 0.091, 0.088); hexolide **2** ($P2_1$) mol. 1 (0.090, 0.117, 0.110), mol 2 (0.100, 0.129, 0.179); hexolide **2** ($C2$) (0.123, 0.086, 0.113). The corresponding differences between hexolide **2** ($P2_1$) mol. 1 and mol. 2 are (0.074, 0.093, 0.128).

REFERENCES

[1] a) D. Seebach U. Brändli, P. Schnurrenberger, M. Przybylski, *Helv. Chim. Acta* **1988**, *71*, 155; b) D. Seebach, S. Roggo, J. Zimmermann, in 'Stereochemistry of Organic and Bioorganic Transformations', Eds. W. Bartmann and K.B. Sharpless, Verlag Chemie, Weinheim, 1987, pp. 85–126, and ref. cit. therein.

[2] a) M. Okada, I. Tajima, H. Sumitomo, *Contemp. Top. Polym. Sci.* **1984**, *4*, 415, and ref. cit. therein; b) M. Okada, I. Tajima, H. Sumitomo, *J. Am. Chem. Soc.* **1979**, *101*, 4013.

[3] a) H. Hirai, K. Naito, T. Hamasaki, M. Goto, H. Koinuma, *Makromol. Chem.* **1984**, *185*, 2347; b) K. Saigo, M. Usui, K. Kikuchi, E. Shimada, T. Mukaiyama, *Bull. Chem. Soc. Jpn.* **1977**, *50*, 1863.

[4] a) A. Collet, *Tetrahedron* **1987**, *43*, 5725; b) J. Canceill, A. Collet, *J. Chem. Soc., Chem. Commun.* **1988**, 582.

[5] a) H.-J. Schneider, R. Busch, *Chem. Ber.* **1986**, *119*, 747; b) H.-J. Schneider, K. Philippi, J. Pöhlmann, *Angew. Chem.* **1984**, *96*, 907; *ibid. Int. Ed.* **1984**, *23*, 908; c) H.-J. Schneider, W. Müller, D. Güttes, *Angew. Chem.* **1984**, *96*, 909; *ibid. Int. Ed.* **1984**, *23*, 911; d) H.-J. Schneider, R. Busch, *Angew. Chem.* **1984**, *96*, 910; *ibid. Int. Ed.* **1984**, *23*, 908.

[6] J. Inanaga, K. Hirata, H. Saeki, T. Katsuki, M. Yamaguchi, *Bull. Chem. Soc. Jpn.* **1979**, *52*, 1989.

[7] D. Seebach, Ph. Renaud, W.B. Schweizer, M.F. Züger, J.-M. Brienne, *Helv. Chim. Acta* **1984**, *67*, 1843.

[8] H. Wynberg, E. G. J. Staring, *J. Am. Chem. Soc.* **1982**, *104*, 166.
[9] D. Seebach, M. F. Züger, *Tetrahedron Lett.* **1984**, *25*, 2747.
[10] a) A. Shanzer, *Bull. Soc. Chim. Belg.* **1983**, *92*, 411; b) A. Shanzer, J. Libmann, F. Frolow, *J. Am. Chem. Soc.* **1981**, *103*, *7339*.
[11] W. J. Considine, *J. Organomet. Chem.* **1966**, *5*, 263.
[12] H. B. Kagan, J. C. Fiaud, *Topics Stereochem.* **1988**, *18*, 249.
[13] C. K. Johnson, ORTEP II, Oak Ridge National Laboratory, Report ORNL-5138, Oak Ridge, Tennessee 37830, USA, 1976.
[14] M. Dobler, 'Ionophores and Their Structures', John Wiley & Sons Inc., New York, 1981.
[15] a) M. Dobler, J. D. Dunitz, B. T. Kilbourn, *Helv. Chim. Acta* **1969**, *52*, 257; b) M. Dobler, R. B. Phizackerley, *ibid.* **1974**, *57*, 664.
[16] a) R. Alper, D. G. Lundgren, R. H. Marchessault, W. A. Cote, *Biopolymers* **1963**, *1*, 545; b) K. Okamura, R. H. Marchessault, in 'Conformation of Biopolymers', Ed. G. N. Ramachandran, Academic Press, London, 1967, Vol. 2, pp. 709; c) J. Cornibert, R. H. Marchessault, *J. Mol. Biol.* **1972**, *71*, 735; d) M. Yokouchi, Y. Chatani, H. Tadokoro, K. Teranishi, H. Tani, *Polymer* **1973**, *14*, 267.
[17] A. McL. Mathieson, *Tetrahedron Lett.* **1965**, 4137.
[18] a) W. B. Schweizer, J. D. Dunitz, *Helv. Chim. Acta* **1982**, *65*, 1547; b) T. H. Keller, E. G. Neeland, S. Rettig, J. Trotter, L. Weiler, *J. Am. Chem. Soc.* **1988**, *110*, 7858.
[19] P. R. Gerber, K. Gubernator, K. Müller, *Helv. Chim. Acta* **1988**, *71*, 1429.
[20] a) P. K. Weiner, P. A. Kollman, *J. Comput. Chem.* **1981**, *2*, 287; b) U. C. Singh, P. K. Weiner, J. W. Caldwell, P. A. Kollman, AMBER (UCSF Version 3.0), Dept. Pharmaceutical Chemistry, University of California, San Francisco, 1986.
[21] S. J. Weiner, P. A. Kollman, D. T. Nguyen, D. A. Case, *J. Comput. Chem.* **1986**, *7*, 230.
[22] M. J. S. Dewar, E. G. Zoebisch, E. F. Healy, J. J. P. Stewart, *J. Am. Chem. Soc.* **1985**, *107*, 3902.
[23] A. Griesbeck, D. Seebach, *Helv. Chim. Acta* **1987**, *70*, 1320.
[24] G. M. Sheldrick, SHELXS-86, 'Crystallographic Computing 3', Eds. G. M. Sheldrick, C. Krüger, and R. Goddard, Oxford University Press, Oxford, 1985, p. 175.
[25] G. M. Sheldrick, SHELX76, System of Computing Programmes, University of Cambridge, Cambridge, England.
[26] J. M. Stewart, G. J. Krüger, H. L. Ammon, C. Dickinson, S. R. Hall, The X-RAY SYSTEM, Computer Science Center, University of Maryland, College Park, Maryland, 1972.